Polymer Chemistry

Chain-growth Click Copolymerization for Synthesis of Branched Copolymers with Tunable Branching Density

Journal:	*Polymer Chemistry*
Manuscript ID	PY-ART-12-2021-001635.R1
Article Type:	Paper
Date Submitted by the Author:	06-Jan-2022
Complete List of Authors:	Ma, Kangling; University of Notre Dame, Department of Chemistry and Biochemistry Jin, Xiuyu; University of Notre Dame, Department of Chemistry and Biochemistry Gan, Weiping; University of Notre Dame, Department of Chemistry and Biochemistry Fan, Chengkai; University of Notre Dame, Department of Chemistry and Biochemistry Gao, Haifeng; University of Notre Dame, Department of Chemistry and Biochemistry

ARTICLE

Chain-growth Click Copolymerization for Synthesis of Branched Copolymers with Tunable Branching Density

Kangling Ma, Xiuyu Jin, Weiping Gan, Chengkai Fan and Haifeng Gao*

Received 00th January 20xx,
Accepted 00th January 20xx

DOI: 10.1039/x0xx00000x

In this work, we reported a facile synthesis of (hyper)branched copolymers with tunable degree of branching (DB) via one-pot chain-growth copper-catalyzed azide-alkyne cycloaddition (CuAAC) reactions. By using a tri-azido core molecule as initiator, a variety of difunctional AB monomers with different linkers were designed for CuAAC copolymerization with a trifunctional AB_2 monomer to produce a series of branched copolymers with tunable compositions and low dispersity. Kinetics study and chain-extension experiments confirmed the features of chain-growth mechanism and living polymerization. Although the AB_2 monomer showed higher homopropagation rate than AB monomers, their copolymerization consumed AB monomer slightly faster than AB_2 monomers probably due to their steric difference. Incorporation of pH-responsive and redox-responsive linkages into AB monomers allowed stimuli-responsive degradation of the branched copolymer structures into fragments. Preliminary studies indicated that branched polymers with lower DB showed higher loading capacity than hyperbranched polymers from homopolymerization of AB_2, demonstrating the dependence of payload encapsulation efficiency on polymer structure compactness. This exploration expanded our toolbox to tune the composition and structures of (hyper)branched polymers for their potential application as unimolecular nanocontainers.

Introduction

(Hyper)branched polymers, a class of three-dimensional globular macromolecules, attracted significant attentions in the past few decades,[1-4] due to their interesting features of easy synthesis, low viscosity, and multiple chain-end functionality.[5-8] Different strategies have been reported to prepare (hyper)branched polymers by using various multifunctional monomers, including AB_m ($m \geq 2$) monomers,[9-11] pairs of A_m and B_n monomers,[12, 13] multivinyl crosslinkers, trifunctional inimers and transfers in self-condensing vinyl polymerization (SCVP),[14-18] and self-condensing ring-opening polymerization.[9, 11, 19] In all these synthesis methods, copolymerization of multifunctional monomers with difunctional monomers provides a practical method to alter the branching density, i.e., degree of branching (DB), of the produced polymers.[20-22]

During the synthesis of (hyper)branched polymers, reactions of the multifunctional monomers often follow step-growth polymerization or the combination of step-growth and chain-growth polymerization mechanism,[2, 23-25] in which random monomer-monomer reactions occur concurrently with polymer-monomer reactions throughout the polymerization processes. As a result, these polymer structures suffer from low molecular weights and very broad molecular weight distribution, which significantly limits their advanced applications as biomaterials,[7] optical materials[26] and catalysts.[27] In this context, exclusive chain-growth synthesis of (hyper)branched copolymers with narrow molecular weight distribution and freely tuned DB represents a desirable endeavour in the field of polymer chemistry. In literature, several strategies have been developed to achieve chain-growth polymerization of AB_m monomers or inimers via slow monomer addition,[10, 28] and reaction-manipulated monomer reactivity,[29-32] in which engineering and/or chemistry methods were applied to selectively favour the monomer-polymer reactions rather than the monomer-monomer reactions. Meanwhile, separate efforts have been reported to achieve tunable DBs of (hyper)branched polymers by varying the ratios of difunctional monomers to multifunctional monomers (e.g., feed ratios of AB and AB_2),[20, 33-35] tuning reaction pressure,[36] or acid catalyst concentrations.[37] However, none of these developments could simultaneously achieve chain-growth polymerization and accurately tuned DB in one system.

Recently, our group developed a one-pot chain-growth polymerization technique by using copper-catalyzed azide-alkyne cycloaddition (CuAAC) reaction.[38] With the introduction of a trifunctional B_3 core molecule, Cu(I) catalyst was complexed at the very beginning and enhanced the reactivity of azido groups on B_3 or B_3-containing polymers. The Cu(I)-containing oligomers served as in-situ generated core with higher reactivity to promote polymer propagation and prevent monomer cross-coupling, leading to a chain-growth polymerization mechanism.[38-40] To date, several AB_2 and AB_3 monomers have been successfully homopolymerized in this CuAAC reactions to produce hyperbranched polymers with DB >

[a] Department of Chemistry and Biochemistry, University of Notre Dame, Notre Dame, Indiana 46556-5670, USA. E-mail: hgao@nd.edu.

Electronic Supplementary Information (ESI) available: [details of any supplementary information available should be included here]. See DOI: 10.1039/x0xx00000x

0.7,[25, 38, 39, 41, 42] although the synthesis of branched copolymers with low DB, has not been available.

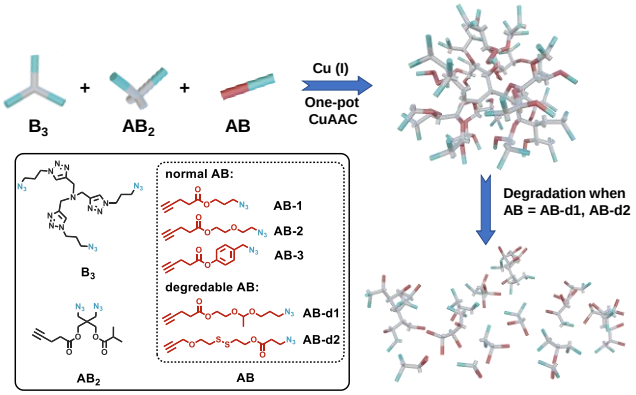

Scheme 1. Chain-growth copolymerization of AB_2 and AB in the use of B_3 core and degradation process of branched copolymers prepared using degradable AB monomers.

Herein, we reported the first one-pot chain-growth copolymerization of AB_2 and AB monomers via CuAAC chemistry and obtained branched copolymers with low dispersity and freely tuned DB. One typical AB_2 monomer 3-azido-2-(azidomethyl)-2-((isobutyryloxy)methyl)propyl pent-4-ynoate was chosen to copolymerize with five AB monomers with different linkers to demonstrate the robust compatibility of monomer compositions (Scheme 1). The DB of synthesized copolymers could be easily tuned from 0 to 0.78 by adjusting the feed ratios of two monomers, while the feature of living chain-growth polymerization was well retained throughout these practices.

Results and Discussion

CuAAC homopolymerization of AB_2 trifunctional monomers has been explored in previous studies to produce hyperbranched polymers with linear increase of molecular weight versus conversion, exhibiting a living chain-growth mechanism with selective polymer-monomer reactions. However, all the produced hyperbranched polymers had densely branched structures with DB > 0.7, which could limit the accessibility of interested payloads to the core domains and affect the property of polymers as unimolecular nanocontainers.[43] Previous attempts from our group introduced external Cu ligands during the CuAAC homopolymerization to adjust the DB values,[25] although the presence of strong ligands compromised the effective confinement of Cu catalyst within the polymers, resulting in concurrent step-growth polymerization mechanism.

In this study, we were interested in the CuAAC copolymerization of AB_2 monomer with difunctional AB monomers containing one alkynyl group and one azido group to tune the polymer branching density without losing the intriguing chain-growth feature. One AB_2 monomer and five AB monomers were designed with their structures shown in Scheme 1 and detailed syntheses in the Supporting Information (Figure S1). As reported earlier, a tris-triazoleamine-based B_3 molecule was used as the core that by complexing with Cu(I) catalyst achieved an increased azido reactivity than monomer and a fast initiation process via selective core-monomer reactions.[39, 44]

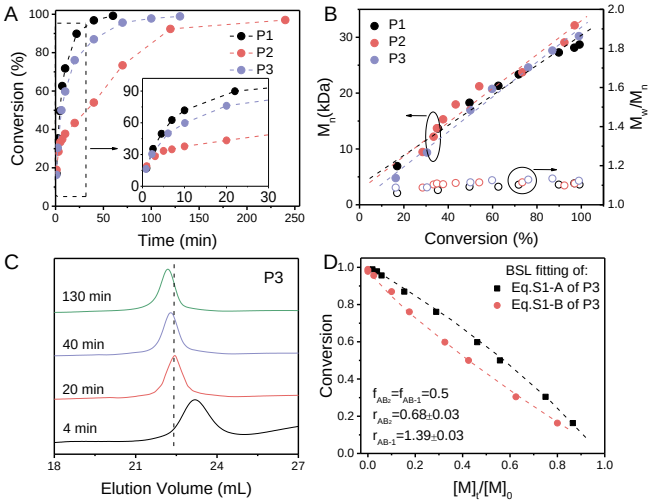

Figure 1. A) Kinetics and (B) evolution of number-average molecular weights (M_n) of polymers in the one-pot CuAAC polymerization at feed ratios of $[monomer(s)]_0:[B_3]_0:[CuSO_4{\cdot}5H_2O]_0:[ascorbic\ acid]_0$ = 200:1:10:20 in DMF at 45 °C, $[monomer(s)]_0$ = 0.5 M; compositions of **P1**-**P3** were listed in Table 1. (C) Stacked SEC traces (RI signal) as a function of reaction time of **P3**: $[AB_2]_0:[AB\text{-}1]_0:[B_3]_0:[CuSO_4{\cdot}5H_2O]_0:[ascorbic\ acid]_0$ = 100:100:1:10:20. The SEC using THF as mobile phase with RI detector based on linear poly(methyl methacrylate) (PMMA) standards. (D) Integrated Beckingham–Sanoja–Lynd (BSL) model fitting of **P3**.

To demonstrate the concept, three CuAAC polymerizations were set up for comparison, including two homopolymerizations and one copolymerization of AB_2 and AB monomers in DMF at 45 °C with the total molar ratio of monomers to B_3 core as $[monomer(s)]_0:[B_3]_0$ = 200:1 (where monomer(s) were AB_2 and/or AB-1, $[AB_2]_0 + [AB\text{-}1]_0$ = 0.5 M). The homopolymerizations of AB_2 and AB-1 reached 96% monomer conversions at 40 min and 4 h, respectively (Figure 1A), in which the monomer conversions were calculated from the ^1H NMR characterization of samples taken out of reactions at timed intervals. When both AB_2 and AB-1 monomers were copolymerized at feed ratio of $[AB_2]_0:[AB\text{-}1]_0:[B_3]_0$ = 100:100:1, the recorded kinetics curve was between those of two homopolymerizations, in which the copolymerization reach 96% conversions of total monomers at 70 min. The produced hyperbranched polymer from homopolymerization of AB_2 monomer and the three-arm star polymer from the homopolymerization of AB-1 monomer showed linear increase of molecular weights with conversion and very low dispersity M_w/M_n = 1.06 and 1.11 (entries **P1** and **P2** in Table 1), respectively. Intriguingly, the copolymerization retained the chain-growth feature and exhibited similar molecular weight increase pace as the two homopolymerizations (Figure 1B). The monomodal elution chromatograms in the size exclusion chromatography (SEC) characterization and their smooth evolution (Figure 1C) indicated the

Table 1. Polymers prepared by CuAAC polymerization of AB_2 and/or AB monomers in the use of B_3 core.

Entry[a]	AB	$[AB_2]_0$:$[AB]_0$:$[B_3]_0$	M_n (kDa)[c]	$M_{n,\ MALLS}$ (kDa)[d]	$M_{n,\ theor.}$ (kDa)[e]	M_w/M_n[c]	D_h (nm)[f]	DB[g]
P1	/	200:0:1	28.7	64.9	67.8	1.06	6.13	0.78
P2	AB-1	0:200:1	32.1	20.7	36.7	1.11	4.85	0
P3	AB-1	100:100:1	26.4	44.1	52.3	1.12	5.63	0.46
P4	AB-1	33:165:1	36.2	25.2	41.5	1.10	6.75	0.13
P5	AB-1	10:190:1	33.0	22.2	38.2	1.11	4.94	< 0.05
P6	AB-1	2:198:1	34.0	21.6	37.1	1.12	5.60	< 0.01
P7	AB-2	100:100:1	24.4	41.6	55.3	1.09	6.59	0.46
P8	AB-3	100:100:1	37.9	49.5	57.1	1.16	7.33	0.42
P9	AB-d1	100:100:1	36.5	/	61.1	1.08	6.55	0.49
P10	AB-d2	100:100:1[b]	42.9	/	63.1	1.20	5.56	0.42
P11	AB-1	150:150:1	31.7	67.9	78.1	1.10	6.43	0.44
P12	AB-1	200:200:1	36.4	93.9	104	1.11	6.87	0.43
P13	AB-1	1000:1000:1	173	488	518	1.08	12.2	0.44
P14	/	900:0:1	71.4	267	303	1.09	8.49	0.78
P15	AB-1	450:450:1	70.2	199	233	1.10	9.05	0.41

a. All polymerizations used conditions of $[B_3]_0$:$[CuSO_4{\cdot}5H_2O]_0$:[ascorbic acid]$_0$ = 1:10:20, $[AB_2]_0$ + $[AB]_0$ = 0.5 M in DMF at 45 °C except stated otherwise. b) $[B_3]_0$:$[CuSO_4{\cdot}5H_2O]_0$:[sodium ascorbate]$_0$ = 1:5:5. c). Apparent number-average molecular weight (M_n) and molecular weight distribution (M_w/M_n) of entries P2, P4, P5, P6, P8, P13-P15 were determined by DMF SEC with RI detector based on linear PMMA standards, other entries were determined by THF SEC with RI detector based on linear PMMA standards. d) Absolute number-average molecular weight ($M_{n,MALLS}$) measured by DMF SEC with a multi-angle laser light scattering (MALLS) detector. e) $M_{n,\ theor} = ([AB_2]_0/[B_3]_0) \times FW_{AB2} + ([AB]_0/[B_3]_0) \times FW_{AB}+FW_{B3}$ as FW_{AB2}, FW_{AB} and FW_{B3} were the formula weights of AB_2, AB and B_3, respectively. f) Hydrodynamic diameter (D_h) was determined by dynamic light scattering (DLS) in the same solvent for SEC measurement. g) The degree of branching (DB) was calculated using the equation DB = 2D/(D + T + L) according to ^{1}H NMR spectra, in which the linear unit (L) and terminal unit (T) were from both the reacted AB_2 and AB monomer units, while the dendritic unit (D) was only from fully reacted AB_2 units.

excellent compatibility of AB_2 and AB-1 in the copolymerization. The conversions of both AB_2 and AB-1 during the copolymerization were then fit into equations S1-A and S1-B (supporting information), which were recently reported as the integrated Beckingham−Sanoja−Lynd (BSL) model and worked well for ideal copolymerization.[45] In Figure 1D, the black dotted curve by fitting overall conversion vs. $[AB_2]_t/[AB_2]_0$ provided $r_{AB\text{-}1}$ = 1.39, while the red dotted curve by fitting overall conversion vs. $[AB\text{-}1]_t/[AB\text{-}1]_0$ determined r_{AB2} = 0.68. The product of $r_{AB\text{-}1}$ and r_{AB2} was close to unity, indicating the current copolymerization systems fitted well with the integrated BSL model. Although the propagation rate of AB_2 in homopolymerization was higher than that of AB-1 (shown in Figure 1A), the reactivity of AB-1 monomer seemed higher than that of AB_2 monomer regarding their reactions with either AB-1 or AB_2 terminated propagating centers (i.e., $r_{AB\text{-}1}$ > 1 and r_{AB2} < 1). This reactivity difference during copolymerization was probably due to the steric difference of the two monomers, in which the bulky AB_2 had lower accessibility than AB-1 to the peripheral azido groups on polymer for CuAAC reaction.[41]

To explore the broad scope of DB tunability, the monomer AB-1 was selected for copolymerization with AB_2 under varied feed ratios but fixed total molar ratio of monomers to initiator ($[AB_2]_0$+$[AB\text{-}1]_0$): $[B_3]_0$ = 200:1. Four copolymerizations with feed ratios of $[AB_2]_0$:$[AB\text{-}1]_0$ from 100:100, 33:165, 10:190 to 2:198 were compared (**P3** – **P6**, Table 1). By increasing the fraction of AB-1 monomer, the polymerizations required longer time to reach > 96% monomer conversions, up to 4 h when only AB-1 was used in **P2**. Figure 2B underscored the linear increase of molecular weight with conversions in these copolymerizations to produce branched copolymers with low dispersity M_w/M_n ~ 1.1 (Figure 2B). At similar monomer conversions, the apparent molecular weights of these four branched copolymers were in the same range because the monomer compositions affected the apparent polymer molecular weight in two opposite directions. On one side, the increased fraction of AB-1 monomer units in polymers decreased the theoretical molecular weight of the branched copolymers due to the lower formula weight of AB-1 monomer than AB_2. On the other side, the increased fraction of AB-1 unit in polymers decreased the structural compactness, i.e., lower DB, which resulted in an enlarged polymer hydrodynamic size in good solvent and a higher apparent molecular weight than higher-DB polymers.

The structure and DB of branched copolymers were determined using the proton nuclear magnetic resonance (^{1}H NMR) spectroscopy. A typical ^{1}H NMR spectrum of **P3** in Figure 3 showed well-resolved peaks with carefully assigned protons from different dendritic (D), terminal (T) and linear (L) units, in which the L units and T units were contributed from both the reacted AB_2 and AB-1 monomers. The DB of the polymer increased from 0 to 0.78 by increasing the AB_2% in the feeding from 0% to 100% (Figure 2C). The hydrodynamic sizes of these polymers were measured by dynamic light scattering (DLS) and exhibited similar values at the range of 4.9 nm to 6.8 nm.

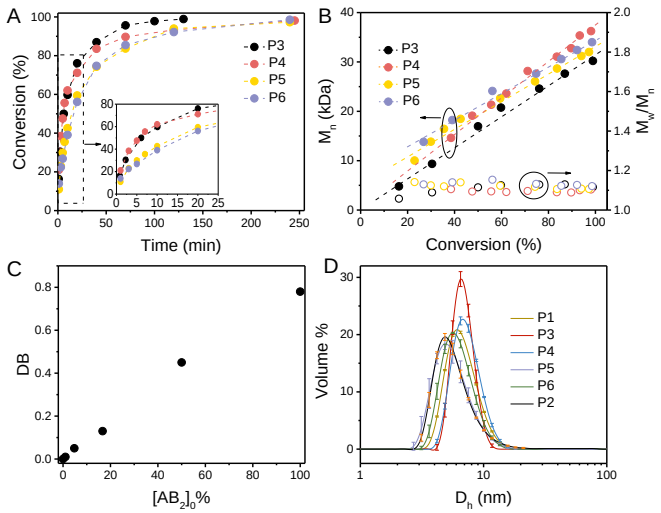

Figure 2. A) Kinetics and B) evolution of number-average molecular weights (M_n) of branched copolymers in the one-pot CuAAC polymerization at feed ratios of $[monomer(s)]_0:[B_3]_0:[CuSO_4{\cdot}5H_2O]_0:[ascorbic\ acid]_0$ = 200:1:10:20 in DMF at 45 °C, $[AB_2]_0+[AB\text{-}1]_0$ = 0.5 M, compositions of **P3**-**P6** were listed in Table 1. C) DB evolution as the function of $[AB_2]_0$% in the feeds. D) DLS traces of two homopolymers and four copolymers with different feed ratios of $[AB_2]_0:[AB\text{-}1]_0$.

To demonstrate the features of living polymerization, selective chain extension reactions were carried out via sequential addition of monomer mixtures in several batches into a one-pot polymerizing system. As an example, when a copolymerization with feed ratio of $[AB_2]_0:[AB\text{-}1]_0:[B_3]_0$ = 100:100:1 approached the complete conversion (> 99%), a mixture of 50 equiv. AB_2 and 50 equiv. AB-1 monomers relative to the original amount of B_3 initiator was added in situ to the

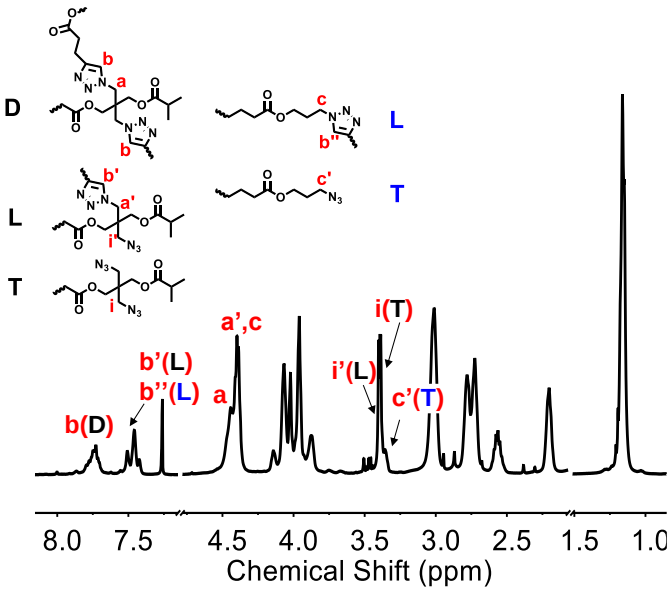

Figure 3. ^{1}H NMR spectrum of copolymer **P3** in $CDCl_3$ at 25 °C.

system to test chain extension. After 2 hours, the 2nd batch monomer reached complete conversion and produced a clean shift of the SEC chromatogram to lower elution volume (Figure 4A). It was discovered that the new elution chromatogram after 2-batch monomer addition completely overlapped with the curve of product from one-batch polymerization at feed ratio of $[AB_2]_0:[AB\text{-}1]_0:[B_3]_0$ = 150:150:1, which confirmed the selective polymer-monomer reactions and clean chain extension of branched macroinitiators in this copolymerization. Similar results were also achieved when comparing the polymers from either one-batch or three-batch monomer addition of total feed ratio of $[AB_2]_0:[AB\text{-}1]_0:[B_3]_0$ = 200:200:1. The hydrodynamic size of these branched copolymers increased with the molecular weight from 5.63 to 6.43 nm and 6.87 nm when the total monomer amount $[AB_2]_0:[AB\text{-}1]_0:[B_3]_0$ increased from 100:100:1 to 150:150:1 and 200:200:1, respectively, regardless the monomers were added in one batch or multiple batches (Figure 4B). This demonstrated feature of living chain-growth polymerization paved the possibility to produce branched copolymers with not only tunable molecular weight and DB, but also layered structure with radially placed segments within one macromolecule.[40]

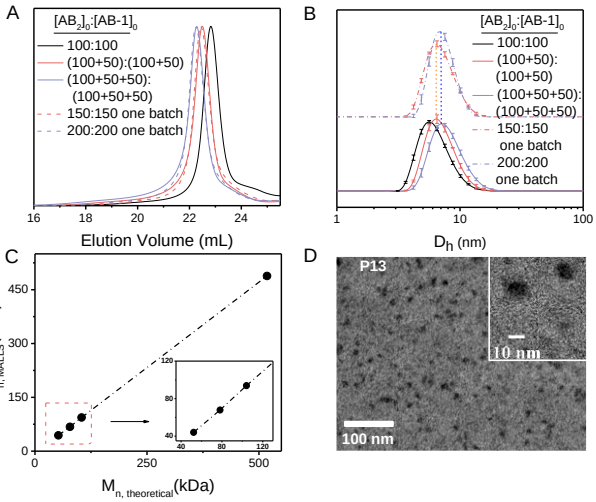

Figure 4. (A) Evolution of SEC curves and (B) hydrodynamic size of copolymers synthesized from one-pot and batchwise monomer-fed CuAAC copolymerization. One-pot reaction: $[AB_2]_0:[AB\text{-}1]_0:[B_3]_0:[CuSO_4{\cdot}5H_2O]_0:[ascorbic\ acid]_0$ = x:x:1:10:20, where x = 150 (**P11**, Table 1) or 200 (**P12**, Table 1) in DMF at 45 °C, $[AB_2]_0+[AB\text{-}1]_0$ = 0.5 M; Batch-wise reaction: first batch $[AB_2]_0:[AB\text{-}1]_0:[B_3]_0:[CuSO_4{\cdot}5H_2O]_0:[ascorbic\ acid]_0$ = 100:100:1:10:20 in DMF at 45 °C, $[AB_2]_0+[AB\text{-}1]_0$ = 0.5 M with the second and the third batches of 50 equiv. of AB_2 and AB-1 monomer (in DMF at $[AB_2]_0+[AB\text{-}1]_0$ = 0.5 M) added at > 99% conversion of the prior batch of AB_2 and AB-1 monomers. C) The plot of $M_{n,MALLS}$ vs $M_{n,theor}$ of branched polymers with different DP. D) TEM image of the branched copolymer **P13** ($[AB_2]_0:[AB\text{-}1]_0:[B_3]_0$ = 1000:1000:1) on a carbon-coated copper grid (mean diameter ca. 12 nm).

Using this technique, a branched copolymer **P13** with targeted degree of polymerization (DP = 2000, $[AB_2]_0:[AB\text{-}1]_0:[B_3]_0$ = 1000:1000:1) and theoretical molecular weight = 488.4 kDa was produced with complete conversion of monomers. The polymer after purification showed an apparent molecular weight M_n = 172.7 kDa and low dispersity M_w/M_n < 1.08 (**P13** and Figure S4). When characterized by MALLS detector connected in DMF SEC, the absolute molecular weight $M_{n,MALLS}$ of **P13** matched very well with the theoretical value (Table 1). In fact, the $M_{n,MALLS}$ values of all

branched copolymers under constant ratio of $[AB_2]_0$:$[AB\text{-}1]_0$ = 1:1 but varied DPs from 200 to 2000 were in linear correlation with the theoretical molecular weights, confirming the living polymerization feature with fast initiation. Meanwhile, the high molecular weight of **P13**, close to half a million allowed direct visualization of individual branched copolymers using transmittance electron microscopy (TEM, Figure 4D), which showed a mean diameter of 12 nm of each individual polymer under dry state. The successful preparation of **P13** suggested the considerable competence of the copolymerization to attain branched copolymer with high molecular weight while the DB controllability maintained.

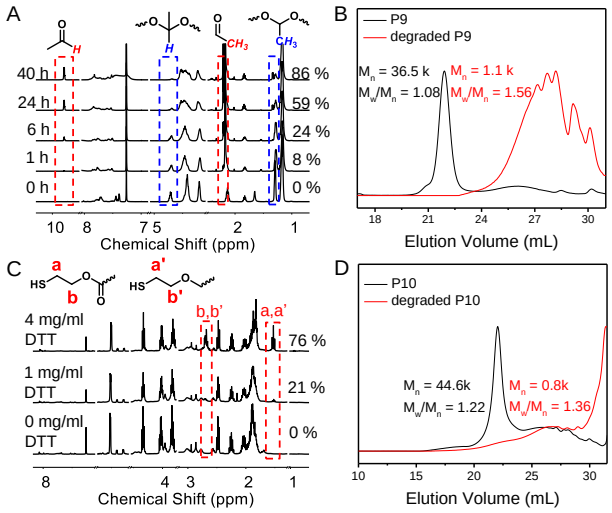

Figure 5. (A) Stacked ^{1}H NMR spectra as a function of time to monitor the degradation of **P9** in $CDCl_3$ with 0.1% CF_3COOH. (B) Comparison of the SEC chromatograms between **P9** and the degraded products. C) Stacked ^{1}H NMR spectra monitoring the degradation of **P10** in $CDCl_3$ at different conditions. D) Comparison of the SEC chromatograms between **P10** and the degraded products.

The thermal properties of homopolymers and copolymers were investigated using thermogravimetric analysis (TGA) and differential scanning calorimetry (DSC). In Figure S5B, all curves showed a first stage < 3 wt% weight loss below 100 °C, which was ascribed to the loss of moisture. During the TGA measurement, the three-arm star polymer **P2** with the least branched structure showed a $T_{d,10\%}$ 100 °C higher than that of hyperbranched polymer **P1** (Table S1). In comparison, the decomposition temperature of copolymer **P3** from 1:1 ratio of AB_2 and AB-1 was between those of the two homopolymers (Figures S5B and S5C). It was interesting to point out that the three glass transition temperatures (T_g) of **P1**, **P2** and **P3** measured by differential scanning calorimetry (DSC, Figure S5A) were very close to each other at around 8 °C, although the monomer compositions were significantly changed from pure AB_2 to AB-1 and their equal molar mixture. This discovery was pretty accidental, it may be used to produce a series of branched copolymers with varied DB, but constant T_g values.

Besides AB-1, four other AB comonomers were also applied in the copolymerization with AB_2. AB-2, a flexible monomer with one more CH_2CH_2O unit and AB-3, a rigid monomer with an aromatic linker, were prepared for copolymerization with AB_2 at the feed ratio of $[AB_2]_0$:$[AB]_0$:$[B_3]_0$= 100:100:1 (**P7** and **P8** in Table 1). Similar to the copolymerization of AB_2 and AB-1, the molecular weights of **P7** and **P8** increased linearly with monomers conversions (Figures S6 and S7) with final polymer products showed low dispersity with M_w/M_n = 1.09 and 1.16, respectively. AB-2, which had similar structure as AB-1 demonstrated the analogous reactivity to prepare **P7** (Figure S6), while the rigid AB-3 presented higher reactivity in **P8** (Figure S7), and the DSC characterization confirmed the more rigid structure of **P8** copolymer as it exhibited a higher T_g = 26 °C than the T_g = 8 °C of copolymers from AB-1.

In addition, two functional AB monomers, termed as AB-d1 and AB-d2, which contained degradable acetal or disulfide linker (Scheme 1) were used to prepare two branched copolymers (**P9** and **P10**, Table 1) with the feed ratio of $[AB_2]_0$:$[AB]_0$:$[B_3]_0$ = 100:100:1, where AB was either AB-d1 or AB-d2. Both copolymerizations were completed within 1 h, produced branched copolymers with linear increase of molecular weight with conversion (Figure S8) and low dispersity. The degradation of acetal-linked copolymer **P9** was carried out in an NMR tube by dissolving 10 mg **P9** in 1 ml $CDCl_3$ containing 0.1% TFA solution. The degradation was monitored in ^{1}H NMR spectroscopy, in which the peaks at 4.71 ppm and 1.30 ppm, assigned to the protons from acetal methine and adjacent methyl groups of the AB-d1 unit exhibited decreased intensity with time. Meanwhile, the peaks at 9.79 ppm and 2.22 ppm belonging to the hydrolysis product acetaldehyde appeared and increased with the progress of degradation. After 2 days, the final degradation product was characterized by THF SEC, which confirmed that only low-molecular-weight fragments were left after 2 days. The M_n decreased from 36.5 kDa to 1.1 kDa and the dispersity increased from 1.08 to 1.56. The degradation of disulfide-linked copolymer **P10** was carried out under two concentrations of dithiothreitol (DTT) using disulfide-thiol exchange reaction, in which 10 mg **P10** was mixed with either 1 mg or 4 mg DTT in 1 ml $CDCl_3$. After 1-day reaction, these two conditions resulted in 21% and 76% disulfide bond breakage in the polymer backbone, respectively. The 76%-degraded **P10** product was further characterized by THF SEC showed a decreased molecular weight from 44.6 kDa to 0.8 kDa, indicating the successful degradation.

To demonstrate how the DB of these branched polymers affect their property as unimolecular nanocontainers, a biocompatible dye, Nile Red (NR) was used as a model guest molecule to evaluate the loading competence of homopolymer and copolymer with the same DP. For this purpose, two polymers, **P14** and **P15**, were selected that had the same DP = 900, but different compositions and branching densities (Table 1). To enable polymer dispersibility in water, **P14** and **P15** after polymerization were further reacted with alkyne-terminated PEG (ay-PEG_{388}) on the periphery azido groups to introduce PEG short chains as the products termed as **P14-PEG** and **P15-PEG**, respectively. The complete conversion of azido groups was demonstrated by Fourier-transform infrared spectroscopy (FTIR, Figure 6B). In a typical loading process. A residue pellet of polymer and NR was prepared by evaporating the solvent of the mixed solution of polymer and NR in hexafluoroisopropanol (HFIP) and reconstituted in aqueous buffer (20 mM HEPES, pH 7.4) with 30 min sonication before centrifugation to remove any unloaded NR. The encapsulated NR was confirmed by the UV-VIS spectroscopy, and the amount was quantified based on NR calibration curve in DMF (Figure S9. Details in the Supporting information).

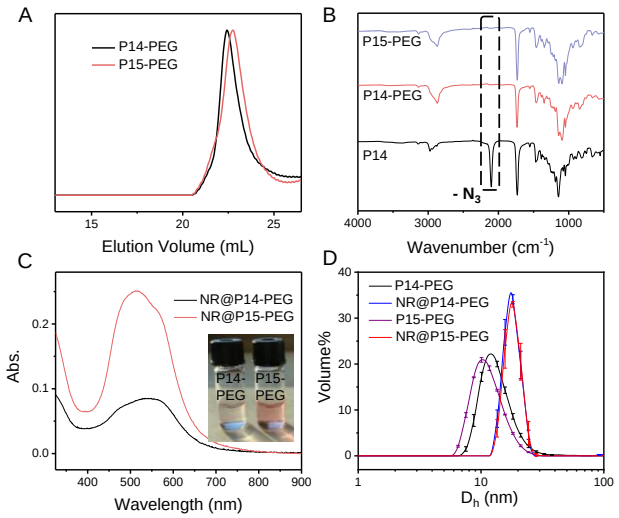

Figure 6. (A) Stacked SEC chromatograms and (B) FTIR spectra of **P14-PEG** and **P15-PEG**. (C) UV-VIS spectra of Nile Red (NR) loaded in **P14-PEG** and **P15-PEG**. (D) DLS traces of **P14-PEG** and **P15-PEG** before and after loading NR in buffer (20 mM HEPES, pH 7.4).

As shown in Figure 6C, broad absorption peaks from NR were observed, indicating the aggregation of NR inside **P14-PEG** and **P15-PEG**. Meanwhile, DLS results (Figure 6D) after loading NR proved that there was no aggregation of polymer, and both **P14-PEG** and **P15-PEG** functioned as unimolecular containers. The NR-loaded samples were freeze-dried and reconstituted in DMF to quantify the amount of encapsulated NR. According to the calibration curve (Figure S9), both the NR loading efficiency and the loading content of **NR@P15-PEG** were about 4 times larger than those of **NR@P14-PEG**. Averagely, there was about 23 NR molecules in one **P15-PEG** nanocontainer, which confirmed the application of this strategy to afford nanocontainer with designed branching density for suitable payloads.

Conclusion

One-pot CuAAC copolymerization of AB_2 and AB monomers were developed to produce branched copolymers with highly regulated DB (from 0 to 0.78) via a chain-growth polymerization mechanism with fast kinetics. Within the studies, the copolymerizations demonstrated living polymerization characteristics that exhibited clean chain-extension and produced branched copolymers with precisely regulated molecular weight, tunable DB values, and low dispersity. Five AB monomers with different compositions were applied for copolymerizations with the AB_2 monomer, demonstrating robust compatibility of the polymerization method in synthesizing degradable polymers. Meanwhile, Nile Red encapsulation experiments using two branched polymers with similar sizes but different DBs demonstrated the influence of branched polymer structures on the dye loading efficiency and content. This work provided a facile tool to synthesize tailor-made branched copolymers with designed branching densities for possible applications as unimolecular nanocontainers.

Conflicts of interest

The authors declare no conflict of interest.

Acknowledgement

The authors thank the National Science Foundation (CHE-1554519) and the ACS Petroleum Research Fund (PRF #59601-ND7) for financial support. K. Ma thanks the support from the Center for Environmental Science and Technology (CEST) at University of Notre Dame for using their facilities.

Reference

1. C. Gao and D. Yan, *Prog. Polym. Sci*, 2004, **29**, 183-275.
2. B. Voit, *J. Polym. Sci. A: Polym. Chem.*, 2000, **38**, 2505-2525.
3. B. Voit, *J. Polym. Sci. A: Polym. Chem.*, 2005, **43**, 2679-2699.
4. A. Qin, J. W. Lam and B. Z. Tang, *Chem. Soc. Rev.*, 2010, **39**, 2522-2544.
5. Y. Zheng, S. Li, Z. Weng and C. Gao, *Chem. Soc. Rev.*, 2015, **44**, 4091-4130.
6. Y. H. Kim, *J. Polym. Sci. A: Polym. Chem.*, 1998, **36**, 1685-1698.
7. T. Cuneo and H. Gao, *Wiley Interdiscip. Rev. Nanomed. Nanobiotechnol.*, 2020, **12**, e1640.
8. H. Han and N. V. Tsarevsky, *Chem. Sci.*, 2014, **5**, 4599-4609.
9. A. Sunder, R. Hanselmann, H. Frey and R. Mülhaupt, *Macromolecules*, 1999, **32**, 4240-4246.
10. P. Bharathi and J. S. Moore, *Macromolecules*, 2000, **33**, 3212-3218.
11. H.-T. Chang and J. M. J. Fréchet, *J. Am. Chem. Soc.*, 1999, **121**, 2313-2314.
12. M. Jikei, S.-H. Chon, M.-a. Kakimoto, S. Kawauchi, T. Imase and J. Watanebe, *Macromolecules*, 1999, **32**, 2061-2064.
13. H. Chen and J. Kong, *Polym. Chem.*, 2016, **7**, 3643-3663.
14. J. M. Frechet, M. Henmi, I. Gitsov, S. Aoshima, M. R. Leduc and R. B. Grubbs, *Science*, 1995, **269**, 1080-1083.
15. D. Yan, A. H. E. Müller and K. Matyjaszewski, *Macromolecules*, 1997, **30**, 7024-7033.
16. K. Matyjaszewski, S. G. Gaynor and A. H. E. Müller, *Macromolecules*, 1997, **30**, 7034-7041.
17. X. Wang and H. Gao, *Polymers*, 2017, **9**, 188–209.
18. J. A. Alfurhood, P. R. Bachler and B. S. Sumerlin, *Polym. Chem.*, 2016, **7**, 3361-3369.
19. D. Yan, J. Hou, X. Zhu, J. J. Kosman and H.-S. Wu, *Macromol. Rapid Commun.*, 2000, **21**, 557-561.
20. A. Ambade and A. Kumar, *Prog. Polym. Sci*, 2000, **25**, 1141-1170.
21. X. Zhu, Y. Zhou and D. Yan, *J. Polym. Sci. B Polym. Phys.*, 2011, **49**, 1277-1286.
22. D. Hölter, A. Burgath and H. Frey, *Acta Polym.*, 1997, **48**, 30-35.
23. A. Sunder, J. Heinemann and H. Frey, *Chem. Eur. J.*, 2000, **6**, 2499-2506.
24. R. Spindler and J. M. J. Frechet, *Macromolecules*, 2002, **26**, 4809-4813.
25. W. Gan, X. Cao, Y. Shi, L. Zou and H. Gao, *J. Polym. Sci. A: Polym. Chem.*, 2018, **56**, 2238-2244.

26. W. Wu, R. Tang, Q. Li and Z. Li, *Chem. Soc. Rev.*, 2015, **44**, 3997-4022.
27. I. N. Kurniasih, J. Keilitz and R. Haag, *Chem. Soc. Rev.*, 2015, **44**, 4145-4164.
28. R. Hanselmann, D. Hölter and H. Frey, *Macromolecules*, 1998, **31**, 3790-3801.
29. F. Li, M. Cao, Y. Feng, R. Liang, X. Fu and M. Zhong, *J. Am. Chem. Soc.*, 2019, **141**, 794-799.
30. Y. Lu, T. Nemoto, M. Tosaka and S. Yamago, *Nat. Commun.*, 2017, **8**, 1863.
31. Y. Ohta, S. Fujii, A. Yokoyama, T. Furuyama, M. Uchiyama and T. Yokozawa, *Angew. Chem. Int. Ed.*, 2009, **48**, 5942-5945.
32. Y. Lu and S. Yamago, *Macromolecules*, 2020, **53**, 3209-3216.
33. S. G. Gaynor, S. Edelman and K. Matyjaszewski, *Macromolecules*, 1996, **29**, 1079-1081.
34. Y. Segawa, T. Higashihara and M. Ueda, *Polym. Chem.*, 2013, **4**, 1746-1759.
35. T. Higashihara, Y. Segawa, W. Sinananwanich and M. Ueda, *Polym. J.*, 2012, **44**, 14-29.
36. Z. Guan, P. M. Cotts, E. F. McCord and S. J. McLain, *Science*, 1999, **283**, 2059-2062.
37. Y. Segawa, T. Higashihara and M. Ueda, *J. Am. Chem. Soc.*, 2010, **132**, 11000-11001.
38. Y. Shi, R. W. Graff, X. Cao, X. Wang and H. Gao, *Angew. Chem. Int. Ed.*, 2015, **54**, 7631-7635.
39. X. Cao, Y. Shi, X. Wang, R. W. Graff and H. Gao, *Macromolecules*, 2016, **49**, 760-766.
40. X. Cao, Y. Shi, W. Gan and H. Gao, *Chem. Eur. J.*, 2018, **24**, 5974-5981.
41. X. Cao, Y. Shi, W. Gan, H. Naguib, X. Wang, R. W. Graff and H. Gao, *Macromolecules*, 2016, **49**, 5342-5349.
42. L. Zou, Y. Shi, X. Cao, W. Gan, X. Wang, R. W. Graff, D. Hu and H. Gao, *Polym. Chem.*, 2016, **7**, 5512-5517.
43. H. Gao, *Macromol. Rapid Commun.*, 2012, **33**, 722-734.
44. W. Gan, X. Cao, Y. Shi and H. Gao, *J. Polym.Sci*, 2020, **58**, 84-90.
45. N. A. Lynd, R. C. Ferrier and B. S. Beckingham, *Macromolecules*, 2019, **52**, 2277-2285.